Electronic Supplementary Information

N-doped $Li_4Ti_5O_{12}$ Nanoflakes Derived from 2D Protonated Titanate for High Performing Anodes in Lithium Ion Batteries

Erwin F. Rodriguez,[a,b] Fang Xia,[b,c] Dehong Chen,*[a] Anthony F. Hollenkamp,[d] and Rachel A. Caruso*[a,b]

dehongc@unimelb.edu.au; rcaruso@unimelb.edu.au

[a]Particulate Fluids Processing Centre, School of Chemistry, The University of Melbourne, Victoria, 3010, Australia.

[b]Manufacturing, The Commonwealth Scientific and Industrial Research Organisation (CSIRO), Clayton, VIC 3168, Australia

[c]School of Engineering and Information Technology, Murdoch University, Murdoch, WA 6150, Australia.

[d]Energy, The Commonwealth Scientific and Industrial Research Organisation (CSIRO), Clayton, VIC 3168, Australia

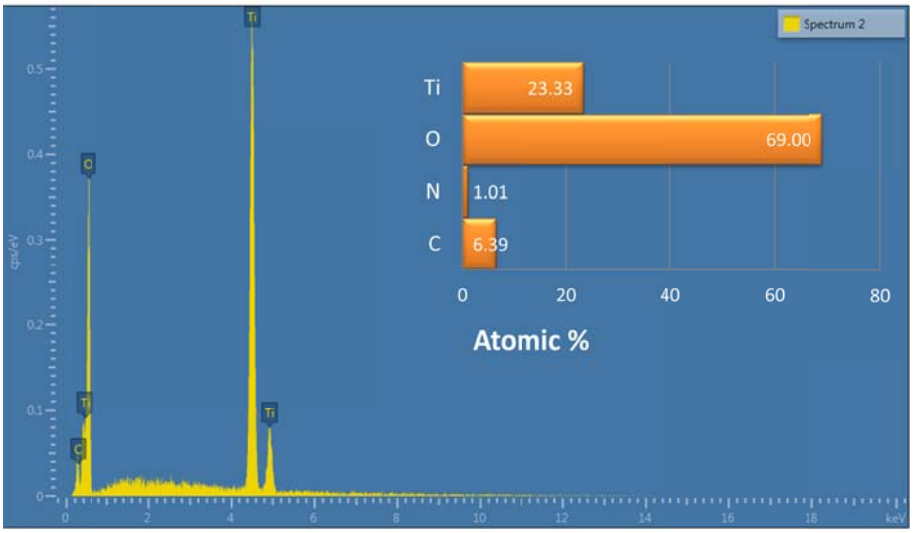

Figure S1. EDS of the dried LHT powder (prior to calcination).

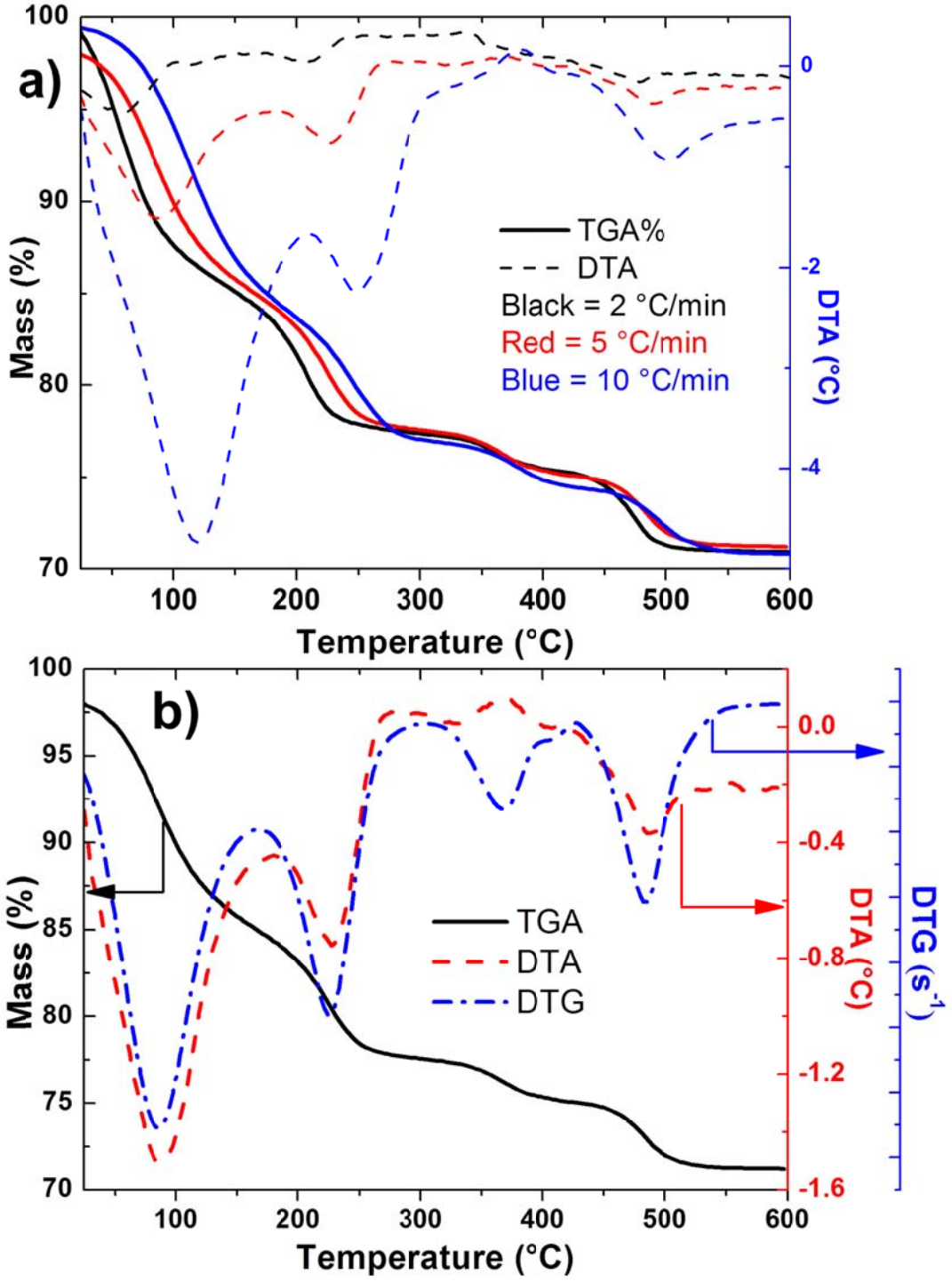

Figure S2. (a) TGA (solid lines) and DTA (dashed lines) curves of LHT heated at 2 (black), 5 (red) and 10 °C min^{-1} (blue). (b) TGA (black), DTA (red) and DTG (blue) curves of LHT heated at 5 °C min^{-1}.

The temperature transition of materials depends on the heating rate, sample size and morphology, and choice of instrumentation, among other things.[1-3] In this study during the

thermal analysis the heating rates were varied (2, 5 and 10 °C min^{-1}), while the other variables were kept constant in order to understand the influence of the heating rate on the LHT to N-LTO phase transition (Figure S2a). Upon increasing the heating rate, not only was the DTA signal intensified, but also the DTA peaks shifted to higher temperatures, whereas the shape of the TGA and DTA curves did not change significantly. Generally, the temperature peak at which the thermal events occur is influenced by the change of the heating rate because of heat and mass transfer hysteresis. For instance, the temperature for the surface water vaporization at a heating rate of 10 °C min^{-1} appeared at approximately 120 °C, but at a 2 °C min^{-1} heating rate, it took place around 58 °C (Figure S2a). At a high heating rate, the peaks in the DTA curves were more intense because of faster release/absorption of energy in a shorter time (exothermic or endothermic thermal events). The same thermal curves were found for all three heating rates (Figure S2a): two endothermic peaks (in the ranges 50-120 °C and 200-270 °C), followed by a small exothermic peak (340-370 °C), and a final endothermic peak (475-520 °C). For the *in situ* HTXRD analysis, a slow heating rate of 2 °C min^{-1} was required because of the limitation on the resolution obtained from the signal collector of the HTXRD.

Figure S2b presents the thermal analysis at a heating rate of 5 °C min^{-1} including the derivative thermogravimetry (DTG) curve, highlighting the similarity of the DTG curve with the DTA curve. Note that the DTG and DTA peaks are almost coincident. For example, the exothermic event at ~369 °C in the DTA curve was reflected in the derivative curve at ~366 °C with a minimal error of 0.8 %. However, it has to be considered that while the DTG peaks pointed downwards, the DTA peaks pointed downwards or upwards, depending on whether the event was endothermic or exothermic. The inflection points of the TGA curve closely coincide with DTA peaks because the maximum rate of loss in mass occurs at the DTA peak with short delay. In this study, DTG was used to interpret the thermal analysis, because the low intensity of the DTA signal at the slow heating rate (2 °C min^{-1}) was easily confused with the noise of the instrument.

Table S1. Stages of the thermal transformation from LHT to N-LTO.

Stage	**Temperature range** (°C)	**Mass loss** (%)	**Temperature Peak** (°C)	**Thermal event at peak**	**Composition at end of stage** [a]
A	25 to 140	~ 14.50	~ 58	Endothermic	LHT·xH$_2$O
B	140 to 280	~ 9.40[b]	~ 208	Endothermic	LHT·0.64H$_2$O
C	280 to 400	~ 2.41[c]	~ 360	Exothermic	LTO·1.60H$_2$O
D	400 to 520	~ 5.90[d]	~ 475	Endothermic	LTO

[a] The composition at the end of the heating stage was estimated by assuming that the nitrogen content was a minor quantity as revealed by both XPS and EDS (Figure 2c and S1), respectively.

[b] Mass loss and composition estimated on the basis of the mass at 140 °C.

[c] Mass loss and composition estimated on the basis of the mass at 305 °C, and assuming the following chemical reaction.

2.5 [$Li_{1.81}H_{0.19}Ti_2O_5$·0.64 H_2O] → $Li_4Ti_5O_{12}$·1.60H_2O + 0.263Li_2O + 0.237H_2O

[d] Mass loss and composition on the basis of the mass at 400 °C.

One by-product could be Li_2O, a solid that has low vapour pressure even at high temperatures. Li_2O can be removed rapidly during calcination when in the presence of oxygen and water.[4] Therefore, a sudden loss of Li_2O and H_2O could explain the small mass decrease during the phase transformation.

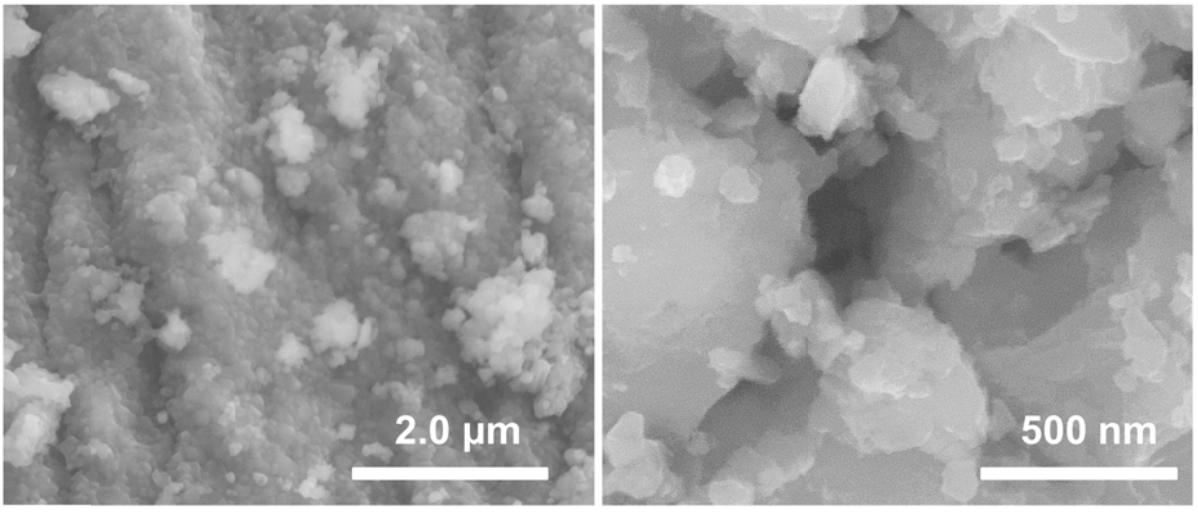

Figure S3. SEM images of the N-LTO after annealing at 700 °C for 2 h under air.

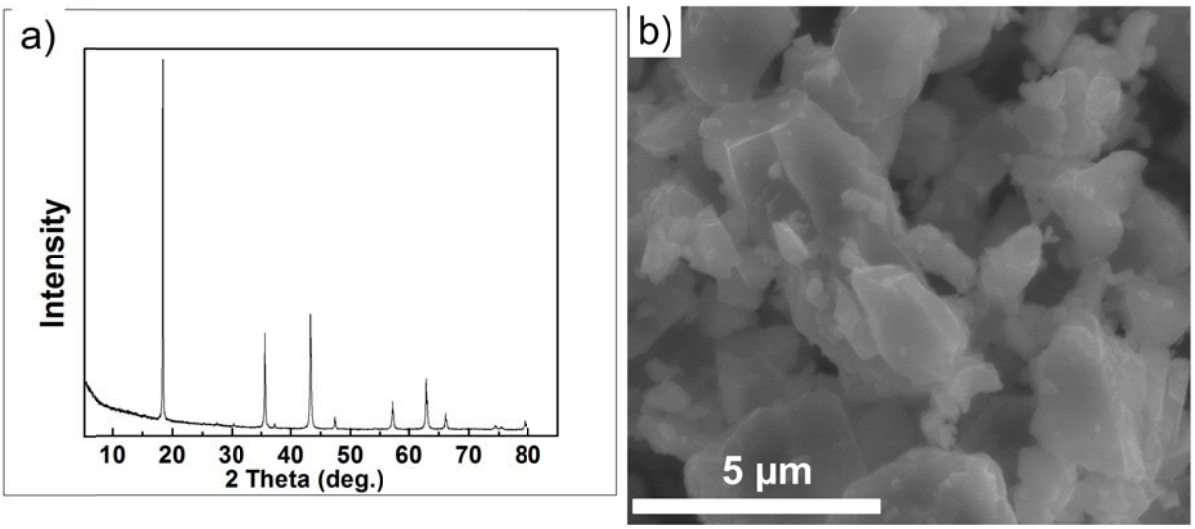

Figure S4. (a) XRD pattern and (b) SEM image of the commercial LTO (com-LTO) used as a control sample in this study.

The sharp reflections of the XRD pattern indicate high crystallinity of this commercial LTO. The com-LTO appeared as coarse-grained particles with a very wide size distribution of the crystal being from a few nanometres to about 5 µm. The com-LTO had a low surface area of 4.3 m^2 g^{-1}.

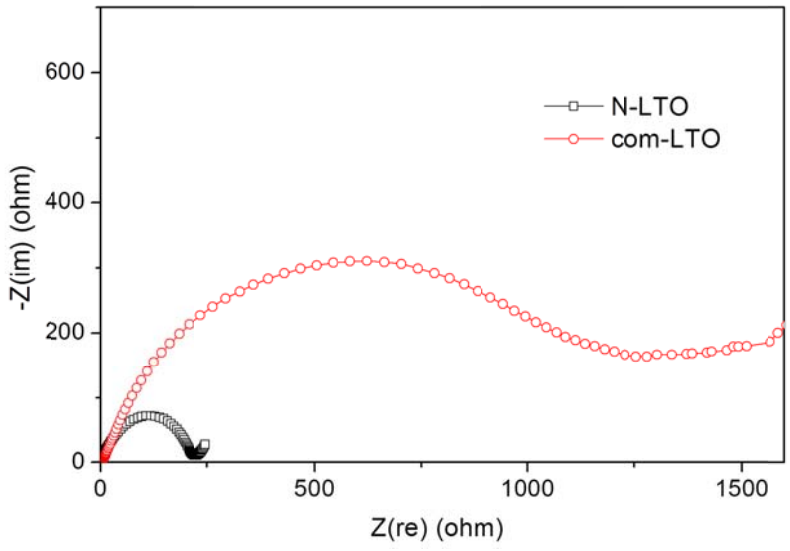

Figure S5. Impedance plane plots at 3.1 V bias voltage for N-LTO and com-LTO, as indicated. The smaller semicircle-diameter of the N-LTO indicates a lower charge transfer resistance compared to com-LTO.

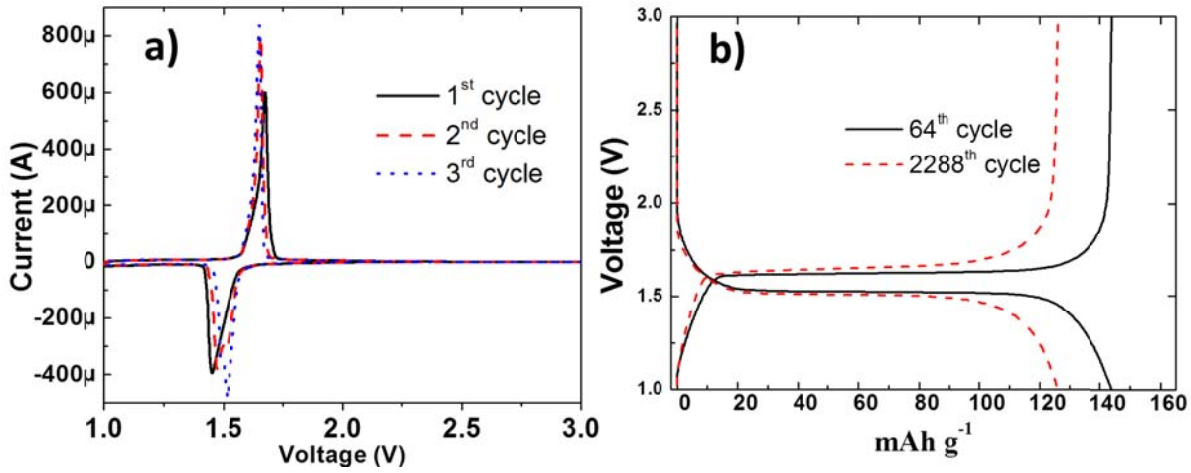

Figure S6. (a) The initial three CV cycles at 0.05 mV s^{-1} voltage sweep rates, and (b) galvanostatic voltage profiles for the indicated cycles of the N-LTO calcined at 550 °C.

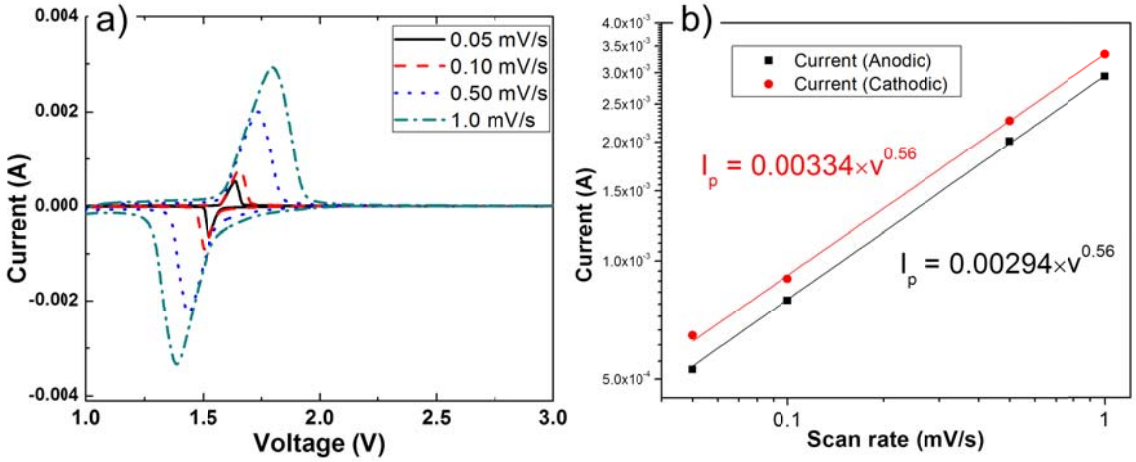

Figure S7. (a) Cyclic voltammograms upon increasing voltage sweep rates, and (b) the relationship between the redox peak currents and the voltage sweep rate of the N-LTO calcined at 550 °C.

1. D. Simatos, G. Blond, G. Roudaut, D. Champion, J. Perez and A. L. Faivre, *J. Therm. Anal.*, 1996, 47, 1419-1436.
2. S. Homer, M. Kelly and L. Day, *Carbohydr. Polym.*, 2014, 108, 1-9.
3. J. C. Van Miltenburg and M. A. Cuevas-Diarte, *Thermochim. Acta*, 1989, 156, 291-297.
4. A. E. Vanarkel, U. Spitsbergen and R. D. Heyding, *Canadian J. Chim.-Rev. Can. Chim.*, 1955, 33, 446-447.